**Proceedings of DETC '02:**
**ASME 2002 International Design Engineering Technical Conferences**
**And Computer and Information in Engineering Conference**
**September 29 – October 2, 2002, Montreal, CANADA**

**DETC02/DAC-XXXXX**

# DRAFT: EMPIRICAL ANALYSIS USING ADVANCED SIMILARITY METHODS

John J. Wood
Department of Mechanical Engineering
Colorado State University
Ft. Collins, CO 80523
jwood@engr.colostate.edu

Kristin L. Wood
Department of Mechanical Engineering
The University of Texas at Austin
Austin, TX 78712

Wade O. Troxell
Department of Mechanical Engineering
Colorado State University
Ft. Collins, CO 80523

## ABSTRACT

Traditional dimensional analysis techniques for predicting the performance characteristics of a product can be greatly improved in both accuracy and domain of applicability by the infusion of empirical data, derived from material tests, into the equations that characterize the system parameters of interest. Advanced similarity methods are investigated which overcome the constraints associated with the traditional methods and provide increased analysis capability and improved insight into the phenomenon governing the problem. Such capability greatly increases the design toolbox available to product developers, across a large range of scale and application. It also significantly enhances a developer's choices for prototype portioning during a development cycle. Solid mechanics and heat transfer applications are used to illustrate the basic utility of the methods.

## INTRODUCTION

The Traditional Similarity Method (TSM) is well understood as a methodology that uses the concept of dimensional analysis, based upon the Buckingham Π theorem, to correlate the respective states of a model and a product. The primary goal of the technique is to allow the prediction of the performance of a product from the measured states of a representative model. This process has been used to save considerable time and expense in contrast to testing complex and expensive full-scale products. Dimensional analysis, theory of dimensions, theory of models, similitude, theory of similarity; all of these terms have been used interchangeably over the past century to describe the process of using the exponents of variables as a starting point for a more detailed dimension-based analysis [1].

Dimensional analysis has long been recognized as a valuable design and analysis tool but has suffered from severe constraints and limits of applicability. Advanced similarity analysis methods, in tandem with recent advances in rapid prototyping technology, have afforded the development of functional testing for geometrically complex physical models [2], free of many of the constraints that limit the application of traditional methods. Until recently, functional tests on rapid prototyped products was rare with the key factor the severe material properties limitations [3].

Advanced similarity methods represent an opportunity to overcome these limitations and those imposed by traditional methods by using scale testing on rapid-prototyped models in concert with advanced similarity prediction techniques. Advanced similarity methods represent a powerful class of analysis tools in development, derived from the basic principles of dimensional analysis. In this paper, the theoretical foundation for traditional dimensional analysis is reviewed to gain a full understanding of the method including constraints and limits of applicability. This review is followed by an introduction to an advanced method, referred to as the Empirical Similarity Method (ESM), to include the derivation of the method and evaluation using both a numerical example and an empirical example to demonstrate the potential of the new methods for empirical engineering analysis.

## BACKGROUND AND MOTIVATION

The generality of dimensional analysis is both its strength and its weakness. With little effort, a partial solution to nearly any problem can be obtained. However, a complete solution and a thorough understanding of the phenomena at work in the problem cannot be obtained. Dimensional analysis has become an important mathematical tool of experimenters, as its greatest asset is the reduction of the number of variables that must be tested in order to formulate or describe a useable function.

Dimensional analysis has the advantage of not requiring a complicated mathematical derivation, but the disadvantage of requiring additional postulates to provide boundaries to the problem at hand. A primary disadvantage to dimensional analysis is that it provides no basis for deciding *a priori* which derived variables are crucial for a particular problem. It has long been recognized, and perhaps best stated by Bridgman [4], that the variables affecting the problem "cannot be decided by the philosopher in his armchair," rather the choice must be made based upon considerable physical experience. Dimensional analysis boasts the ability to predict results without an understanding or even knowledge of the governing fundamental equations and often provides acceptable results without expensive or complex computational models.

The origin of dimensional analysis can be traced back to the ancient Greeks and their use of basic principles of geometric similarity, ratio, and proportionality. Early in the 17th century Galileo used these fundamental principles in his attempts to characterize and predict the failure of beams [5]. Although other scientists recognized the value of units, Baron Jean-Baptiste Fourier was certainly one of the first scientists to apply and document the concept of "dimensions" or "fundamental units" to actual quantities and, as a result, is often referred to as the founder of dimensional analysis [6]. The ideas first formalized by Fourier were applied with great success at the end of the 19th century. During the 1900-1920 timeframe, physicists attempted to determine the limitations of the newly introduced methods by clarifying the assumptions required for the successful application of dimensional analysis. In 1914, Buckingham gave the first generally accepted proof of the Π Theorem [5]. His publications came at a time when physicists were just becoming aware of the power of the theorem and, as such, Buckingham is often recognized as the founder of the newly labeled Buckingham Pi Theorem.

Lord Rayleigh was another major contributor to the advancement of the methods of dimensional analysis [6]. In 1915 Rayleigh published his method of indices, which attempted to take the next step in considering similitude as a method for comparison between the states of two similar systems. This work, along with Buckingham's Π Theorem were combined by Bridgman in 1922 and formalized into what is now known as dimensional analysis [1].

## TRADITIONAL SIMILARITY METHOD

Dimensional analysis provides a qualitative relationship; however, when combined with experimental results or procedures, it provides quantitative results as well as prediction equations within recognized limitations [7]. The principal advantage to dimensional analysis lies in reducing the number of variables that must be investigated and in formulating advantageous dimensionless variables known as Π terms. The number of Π terms required to express a relationship among the variables in any phenomenon is equal to the number of quantities involved, minus the rank of the dimensional matrix [8] (an expression of the number of independent fundamental dimensions). In equation form [7]:

$$N = n - b \qquad \text{(Eq. 1)}$$

where: $N$ – number of π terms
$n$ – total number of quantities involved
$b$ – number of basic dimensions involved

The only restriction on the Π terms is that they be dimensionless and independent.

The fundamental premise of the TSM and the limitations in its application can best be understood by considering the mathematical foundations of the method. We begin by considering the model and product systems, both comprised of relevant physical parameters ($q_i$), which characterize the respective systems. The two systems are described by the following complete and homogeneous equations:

$$f\left(q_{m,1}, q_{m,2}, \ldots, q_{m,n}\right) = 0$$
$$g\left(q_{p,1}, q_{p,2}, \ldots, q_{p,n}\right) = 0$$

where the subscripts $m$ and $p$ denote the scaled model and product parameters respectively. The Buckingham Π theorem states that a complete equation written in terms of dimensional system parameters $q_j$, j = 1, …, $n$, can be recast in terms of dimensionless parameters $\pi_i$, i = 1, …, $N$, where $N < n$ as described in Equation 1. By applying the Π theorem, the above system of equations can be equivalently represented in terms of the Π terms as:

$$F\left(\pi_{m,1}, \pi_{m,2}, \ldots, \pi_{m,N}\right) = 0$$
$$G\left(\pi_{p,1}, \pi_{p,2}, \ldots, \pi_{p,N}\right) = 0$$

One can refer to [9] for a systematic derivation of the dimensionless parameters.

Any physical phenomena can be described by a complete homogeneous equation (e.g. drag on a ship, stress in a shaft,

etc.) [10] as demonstrated in the following example where the fundamental dimensions of force (F) and length (L) are chosen. Consider the variables involved in characterizing the deflection and normal stress on a tapered cantilevered beam:

| Variable | Symbol | Dimensions |
|---|---|---|
| Applied Load | $P$ | F |
| Beam Length | $L$ | L |
| Modulus | $E$ | $FL^{-2}$ |
| Density | $\rho$ | $FL^{-3}$ |
| Normal Stress | $\sigma$ | $FL^{-2}$ |
| Root Height | $h_r$ | L |
| Root Width | $b_r$ | L |
| Tip Height | $h_t$ | L |
| Tip Width | $b_t$ | L |

A product, π, of these variables will have the following form [10]:

$$\pi = f\left(P, L, E, \rho, \sigma, h_r, b_r, h_t, b_t\right)$$
$$\pi = P^{k1} L^{k2} E^{k3} \rho^{k4} \sigma^{k5} h_r^{\ k6} b_r^{\ k7} h_t^{\ k8} b_t^{\ k9}$$

The dimensions of π (denoted by brackets around the variable) must be:

$$[\pi] = [F]^{k1}[L]^{k2}\left[FL^{-2}\right]^{k3}\left[FL^{-3}\right]^{k4}\left[FL^{-2}\right]^{k5} [L]^{k6}[L]^{k7}[L]^{k8}[L]^{k9}$$

$$[\pi] = [F]^{k1+k3+k4+k5}[L]^{k2-2k3-3k4-2k5+k6+k7+k8+k9}$$

Since π is required to be dimensionless; the exponents of each of the fundamental variables (F and L) must be zero. Therefore, any solution to the following set of linear equations is a set of exponents in a viable dimensionless product π.

$$k1 + k3 + k4 + k5 = 0$$
$$k2 - 2k3 - 3k4 - 2k5 + k6 + k7 + k8 + k9 = 0$$

A century of research has provided us with several efficient methods to solve the above equations to obtain a combination of exponents that will provide useful sets of variables we can use to compare the equality of two systems. A completely similar system results when all Π terms ($\pi_1, \pi_2, ..., \pi_N$) are the same for both the model and the product since a complete set of dimensionless products determines all dimensionless products of the given variables [10]. Here we will use the echelon matrix formulation [7, 9] to obtain a set of Π terms for analysis of the stated tapered beam problem. The original dimensional matrix is shown in Table 1.

Table 1. Cantilevered Tapered Beam Dimensional Matrix

| **Fundamental Dimensions** | **P** | **L** | **E** | | | | | | |
|---|---|---|---|---|---|---|---|---|---|
| | **P** | **L** | **E** | **ρ** | **σ** | **$h_r$** | **$b_r$** | **$h_t$** | **$b_t$** |
| F | 1 | 0 | 1 | 1 | 1 | 0 | 0 | 0 | 0 |
| **L** | 0 | 1 | -2 | -3 | -2 | 1 | 1 | 1 | 1 |

Due to the choice of fundamental dimensions of F and L, the matrix in Table 1 is already in Echelon form, and we can therefore proceed with derivation of the Π terms. From the matrix in Table 1, we obtain the following Π terms:

$$\pi_1 = EL^2 / P \qquad \pi_5 = b_r / L$$
$$\pi_2 = \rho L^3 / P \qquad \pi_6 = h_t / L$$
$$\pi_3 = \sigma L^2 / P \qquad \pi_7 = b_t / L$$
$$\pi_4 = h_r / L$$

The dimensionless parameters, or Π terms, containing the state of interest of the two systems can now be described explicitly in terms of the other dimensionless parameters as:

$$\pi_{m,x} = f\left(\pi_{m,1}, \pi_{m,2}, ..., \pi_{m,N-1}\right) = 0$$
$$\pi_{p,x} = g\left(\pi_{p,1}, \pi_{p,2}, ..., \pi_{p,N-1}\right) = 0$$

From this set of equations, it can be said that $\pi_{m,x}$ and $\pi_{p,x}$ are identical, if $\pi_{m,i} = \pi_{p,i}$ for all $i$ = 1, 2, …, *N-1*. As a result, the states of the model and the product can be correlated based upon the following derived equation:

$$\pi_{m,x}\left(Q_m\right) = \pi_{p,x}\left(Q_p\right) \qquad \text{(Eq. 2)}$$

Equation 2 represents the prediction equation correlating a Π term for the model with the same Π term for the product or $\Pi i_m = \Pi i_p$. (subscripts *i* seem incorrectly formatted) This correlation is only valid if the following equation is also true:

$$\pi_{m,i}\left(Q_m\right) = \pi_{p,i}\left(Q_p\right), \forall i = 1,2,..., N-1 \qquad \text{(Eq. 3)}$$

Equation 3 represents the similarity constraints that must be satisfied for the prediction to be valid. The prediction equation coupled with the similarity constraints form the fundamental basis of the TSM. In order to predict the state of a product using the above prediction equation, the model should be designed such that all of the similarity constraints are satisfied. If all the similarity constraints for a model-product pair are satisfied, the system is defined as well-scaled. If, however, any of the similarity constraints are not satisfied, the system is defined as distorted, and the TSM may provide inaccurate predictions as a result.

Often it is not feasible to impose complete similarity in a model test [11]. When one or more of the dimensionless products (i.e. Π terms) is not equal for the model and product, distortion of the problem occurs. Distortion of the model can be caused by a number of phenomena including [7]:

- Unavailability of proper modeling materials
- Required model details may impose excessive fabrication costs
- Available testing equipment may not meet test requirements (e.g. wind tunnel speeds, temperatures, etc.)
- Failure to include critical problem variables in the analysis

Distortion of the model-product pair is defined simply as:

$$\Pi_{ip} \neq \Pi_{im}$$

As mentioned previously, the generality of dimensional analysis makes it an easy method to apply but also severely limits its application. The method is extremely susceptible to geometric, material, and boundary condition distortions between the model and product. Such challenges make model predictions using rapid-prototypes with the TSM extremely difficult and have caused the utility and reliability of scale testing results to be challenged frequently [9].

## EMPIRICAL SIMILARITY METHODS

As we have seen it can be very difficult to characterize the performance of a designed product by performing tests on a prototype model due to the severe constraints imposed by the required similarity conditions that are often impractical or impossible to satisfy. With the recognized deficiencies of the TSM, we seek to discover methods to provide improved prediction accuracy and also to increase the range of applicability and/or decrease the constraints required for an accurate prediction. This section begins with a review of the current state of ESMs with the intent to identify specific areas where the current methods are both successful and deficient and to pave the way for the next advancement in the method. The first two methods described were developed by Cho, et al. [12], and the third is a new method proposed which has shown improvement over the previous methods in efficiency of application, prediction accuracy, and insight into the degree of model distortion. The task, as in TSM, is to determine the transformation required to get from the model state to successful prediction of the product as shown in Figure 1. While the TSM uses a single multiplication factor for this transformation, derived from the appropriate Π term, the ESM takes a different approach.

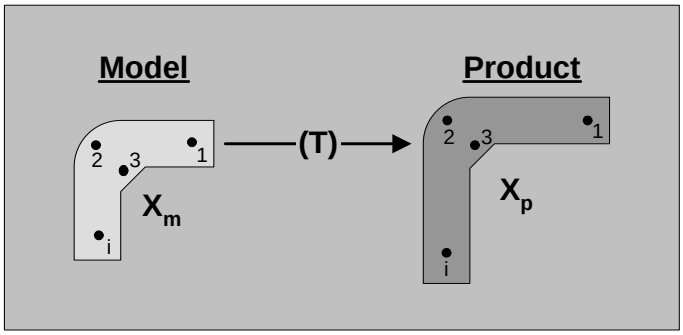


Figure 1. Transformation from Model to Product.

The ESM [2] is viewed as a 2-phase process that uses state vector transformations in 2 distinct parameter spaces, material ([M]) and geometry ([G]), to transform the state of a predictive model ( $\vec{X}_m$ ) to that of a product ( $\vec{X}_p$ ). In the derivation of the two transformations, they are assumed to be orthogonal and can therefore be considered independently. Our orthogonal assumption allows the consideration of the material transformation independent of any complexities associated with the geometry. With this in mind, we seek to simplify the determination of the material transformation by simplifying the geometry of the model and product through the introduction of representative specimens used specifically to derive the material transformation. As such the model and product specimens are constructed using the same materials, and the same processes where appropriate, as the model and product respectively. Although research to envelope the degree of geometric similarity required from the specimens is ongoing, for the purpose of this paper, we limit the geometric deviations to product specimens that retain the same basic relative dimensions but do not require complex machining to manufacture.

Figure 2 graphically depicts the ESM process with its now four distinct vector states of parameter values as shown below. The states of interest studied thus far have been limited to temperature, beam stress, beam deflection, and angle of beam rotation. Research into the predictive capabilities of the methods in other product domains is planned; however, the general ESM approach should be applicable to any domain as long as its basic mathematical assumptions are satisfied.

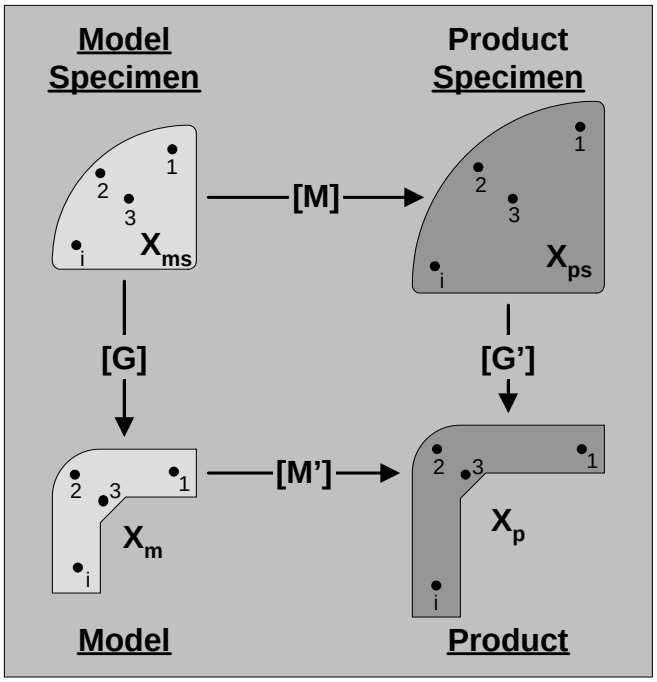


Figure 2. Data Points and Transformation Matrices.

$$\vec{X}_{ms} = \begin{bmatrix} X_{ms,1} \\ X_{ms,2} \\ \vdots \\ X_{ms,i} \end{bmatrix} \qquad \vec{X}_{ps} = \begin{bmatrix} X_{ps,1} \\ X_{ps,2} \\ \vdots \\ X_{ps,i} \end{bmatrix}$$

$$\vec{X}_{m} = \begin{bmatrix} X_{m,1} \\ X_{m,2} \\ \vdots \\ X_{m,i} \end{bmatrix} \qquad \vec{X}_{p} = \begin{bmatrix} X_{p,1} \\ X_{p,2} \\ \vdots \\ X_{p,i} \end{bmatrix}$$

The goal of the ESM is to be able to accurately predict the state of a product ( $\vec{X}_p$ ) from the measured states of the model specimen, product specimen and model ( $\vec{X}_{ms}$, $\vec{X}_{ps}$, $\vec{X}_m$ ) according to the following generic formulation:

$$\vec{X}_p = f\left(\vec{X}_{ms}, \vec{X}_{ps}, \vec{X}_m\right)$$

Phase 1 – This phase involves the physical testing of a model specimen and product specimen, manufactured from the model and product material respectively, to empirically abstract a geometry independent material transformation matrix [M], based upon the measured states of the model specimen ( $\vec{X}_{ms}$ ) and the product specimen ( $\vec{X}_{ps}$ ) (see Figure 2). The transformation matrix is also referred to as a *scale* matrix as a result of the identical geometrical shape, but potentially variable scale, of the specimen pair.

Phase 2 – This phase involves the physical testing of the model specimen and a product replica model, both manufactured from the model material, to empirically abstract a material independent geometrical transformation matrix [G], based upon the measured states of the model specimen ( $\vec{X}_{ms}$ ) and model ( $\vec{X}_m$ ) (see Figure 2). The transformation matrix is also referred to as a *form* matrix as a result of the intent of the matrix to capture the purely geometrical characteristics of the transformation.

The ESM has resulted in the derivation of the following previously developed methods for the prediction of a product's performance [2]:

- Psuedo-Inverse Method
- Circulent Matrix Method

In addition, the following method has been developed which shows extremely promising results in the efficiency of its application, prediction accuracy, and advanced insight into the degree of model distortion and the error in product predictions.

- Compensation Matrix Method

The Psuedo-Inverse and Circulent matrix methods each contain two variant solutions that correspond to the two possible solution paths, Paths A and B, shown in Figure 3.

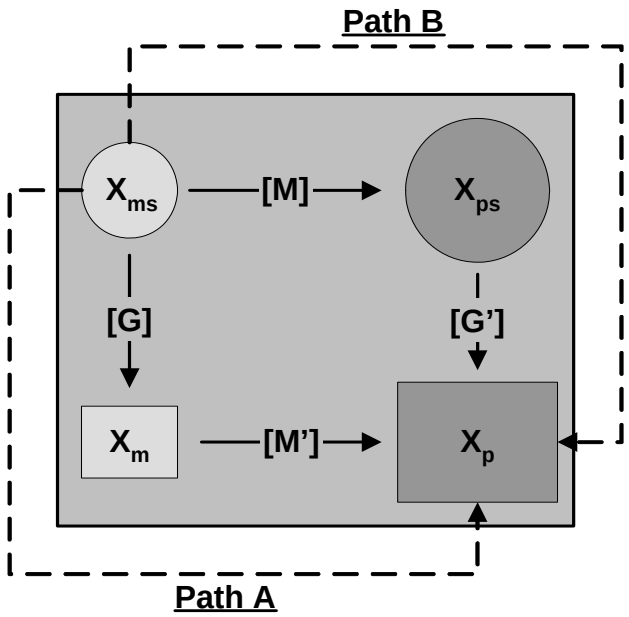

Figure 3: Possible Solution Paths from $\vec{X}_{ms}$ to $\vec{X}_{p}$.

Path A represents the process of using the phase 1 derived specimen scale transformation matrix [M] as an approximation for the model transformation matrix [M']. This transformation is applied to the model state vector ( $\vec{X}_{m}$ ) for the prediction of the product state vector ( $\vec{X}_{p}$ ) as follows:

$$\vec{X}_{ps} = [M]\vec{X}_{ms} \quad \text{(Eq. 4)}$$

$$[M] = \vec{X}_{ps}\vec{X}_{ms}^{-1} \quad \text{(Eq. 5)}$$

$$\vec{X}_{p} = [M']\vec{X}_{m} \quad \text{(Eq. 6)}$$

$$\vec{X}_{p} \cong [M]\vec{X}_{m} \quad \text{(Eq. 7)}$$

Path B represents the process of using the phase 2 derived model form transformation matrix [G] as an approximation for the product form transformation matrix [G']. This transformation is applied to the product specimen state vector ( $\vec{X}_{ps}$ ) for the prediction of the product state vector ( $\vec{X}_{p}$ ) as follows:

$$\vec{X}_{m} = [G]\vec{X}_{ms} \quad \text{(Eq. 8)}$$

$$[G] = \vec{X}_{m}\vec{X}_{ms}^{-1} \quad \text{(Eq. 9)}$$

$$\vec{X}_{p} = [G']\vec{X}_{ps} \quad \text{(Eq. 10)}$$

$$\vec{X}_{p} \cong [G]\vec{X}_{ps} \quad \text{(Eq. 11)}$$

With this background as a foundation we now proceed to derive each of the methods and attempt an evaluation of each based upon their own merits, limitations, and ability to accurately predict the state of a product.

## PSUEDO-INVERSE MATRIX APPROACH:

As described above, two paths exist to get from the state vector of the model specimen ( $\vec{X}_{ms}$ ) to the state vector of the product ( $\vec{X}_{p}$ ) as shown in Figure 3. Equations 5 and 9 above provide the following derivations for the material and geometry transformations from the known vector states:

$$[M] = \vec{X}_{ps}\vec{X}_{ms}^{-1}$$
$$[G] = \vec{X}_{m}\vec{X}_{ms}^{-1}$$

However, the state vector $\vec{X}_{ms}$ is most often a *n* x 1 vector for which the inverse is not defined unless *n* = 1. We therefore propose a substitution for the inverse ( $\vec{X}_{ms}^{-1}$ ) with the psuedo-inverse ( $\vec{X}_{ms}^{+}$ ) defined as the *n* x 1 Moore-Penrose pseudo inverse [13] of $\vec{X}_{ms}$ where $\vec{X}_{ms}^{+} \equiv \left(\vec{X}_{ms}^{T}\vec{X}_{ms}\right)^{-1}\vec{X}_{ms}^{T}$. This substitution results in the following modified transformations:

$$[M] = \vec{X}_{ps}\vec{X}_{ms}^{+} \quad \text{(Eq. 12)}$$

$$[G] = \vec{X}_{m}\vec{X}_{ms}^{+} \quad \text{(Eq. 13)}$$

Substitution of Equations 4 and 8 into Equations 11 and 7 respectively results in the following expressions representing the two solution paths A and B:

$$X_{p} \cong [G]\cdot[M]X_{ms}$$
$$X_{p} \cong [M]\cdot[G]X_{ms}$$

In order to maximize our confidence in the above equations predicting the solution state vector $\vec{X}_{p}$, the above expressions should provide near equal results. Failure to provide near equal results is a strong indicator that distortion in one or both of the paths, and thus in [M] or [G], is preventing convergence of the solution. In contrast, if the above equations provide the same result, the following expression will be true:

$$[G]\cdot[M] = [M]\cdot[G]$$

As a result the following transformation matrices are said to be approximately equal:

$$[M] = [M']$$
$$[G] = [G']$$

This equality of transformation matrices indicates that either the specimen pair and the model-product pair have been designed in accordance with the same similarity laws ([M] = [M']) or they exhibit an equal degree of distortion, which is

extremely unlikely. Likewise the model family and the product family have also either been designed in accordance with the same similarity laws ([G] = [G']) or they also exhibit an equal degree of distortion, again, not likely. If we proceed with the derivation on this assumption, we are soon faced with another problem characteristic of the Psuedo-Inverse method. Equations 5 and 9 define the scale and form matrices [M] and [G]. However, given state vectors $\vec{X}_{ms}$, $\vec{X}_{ps}$, and $\vec{X}_{m}$, each containing *n* elements or data points; we are presented with [M] and [G] matrices containing $n^2$ unknowns with only *n* equations available for their solution. The resulting matrices are not unique when n > 1 unless the number of columns in the state vectors $\geq$ the number of rows. The number of rows in the state vectors (designated *n*) typically represents the number of test points for the specimens and model and the number of points being predicted on the product. The number of columns in the state vectors (designated *m*) represents the number of specimens or individual specimen tests conducted. Up to this point we have assumed m = 1 and will continue with this assumption in the evaluation of each method to provide an equal basis for comparison.

To demonstrate this non-uniqueness consider the following derivation of the scale matrix [M] given test data representing the temperature at corresponding points on the specimens:

$$[T_{ms}] = \begin{bmatrix} 450 \\ 400 \\ 365 \end{bmatrix} \qquad [T_{ps}] = \begin{bmatrix} 600 \\ 500 \\ 428 \end{bmatrix}$$

$$[M] = \vec{T}_{ps}\vec{T}_{ms}^{\,+} \qquad \text{where:} \qquad \vec{T}_{ms}^{\,+} \equiv \left(\vec{T}_{ms}^{\,T}\vec{T}_{ms}\right)^{-1}\vec{T}_{ms}^{\,T}$$

Reference: [13]

$$\rightarrow \quad [M] = \begin{bmatrix} 0.545 & 0.484 & 0.442 \\ 0.454 & 0.403 & 0.368 \\ 0.389 & 0.345 & 0.315 \end{bmatrix}$$

However, the following scale matrix is also a solution as are many others:

$$\rightarrow \quad [M] = \begin{bmatrix} 0.5 & 0.5 & 0.476 \\ 0.1 & 1.0 & 0.15 \\ 0.5 & 0.5 & 0.0082 \end{bmatrix}$$

Thus far we have shown that the Psuedo-Inverse method is unable to derive a unique scale and form transformation matrix from a single set of data points. In addition, empirical tests conducted thus far using this method have shown sensitivity to distortion which manifests itself in significant differences between the transformation matrices [M] and [M'] as well as [G] and [G'] from Figure 2. The ability of the method to predict the product state is dependent upon the similarity of these transformation matrices, and any differences will have a direct impact on the accuracy of the prediction method. These insights lead to the conclusion that this method is susceptible to errors in predicting the state of a product. One way the issue of uniqueness could be alleviated is with additional sets of specimen and model test data. As we have seen, in order to obtain a unique solution, the number of tests required would be equal to or greater than the number of data points being investigated which would greatly reduce the efficiency of the method. The inability to derive a unique form and scale matrix from a single set of data points is a significant hindrance of the Psuedo-Inverse method. As a result, we look for a method that will provide a unique transformation matrix from a single set of data.

## CIRCULENT MATRIX APPROACH:

Cho proposed a modification to the state vectors ($\vec{X}_{ms}$, $\vec{X}_{ps}$, and $\vec{X}_{m}$) that converts them to their equivalent circulent matrices. There are two initial benefits to be gained in using this method based solely upon the mathematical formulation. The first is the resulting derived transformation matrices [M] and [G] will be uniquely determined. Secondly, since the circulent state matrices are, by definition, square, the psuedo-inverse is no longer required as the matrix inverse is applicable in all cases where cir($\vec{X}_{ms}$) is invertible. The special properties of the circulent matrix result in a transformation matrix limited to just *n* unknown coefficients that can be solved uniquely. The circulent matrix is defined as follows:

$$[X] = \begin{bmatrix} X_1 \\ X_2 \\ X_3 \\ \vdots \\ X_n \end{bmatrix} \rightarrow cir(\vec{X}) = \begin{bmatrix} X_1 & X_n & X_{n-1} & \cdots & X_2 \\ X_2 & X_1 & X_n & \cdots & X_3 \\ X_3 & X_2 & X_1 & \cdots & X_4 \\ \vdots & \vdots & \vdots & \ddots & \vdots \\ X_n & X_{n-1} & X_{n-2} & \cdots & X_1 \end{bmatrix}$$

By way of example, applying this equation to the state vector for the model specimen results in the following matrix;

$$cir(\vec{X}_{ms}) = \begin{bmatrix} X_{ms,1} & X_{ms,n} & X_{ms,n-1} & \cdots & X_{ms,2} \\ X_{ms,2} & X_{ms,1} & X_{ms,n} & \cdots & X_{ms,3} \\ X_{ms,3} & X_{ms,2} & X_{ms,1} & \cdots & X_{ms,4} \\ \vdots & \vdots & \vdots & \ddots & \vdots \\ X_{ms,n} & X_{ms,n-1} & X_{ms,n-2} & \cdots & X_{ms,1} \end{bmatrix}$$

By converting the state vectors to their equivalent circulent matrices, we derive the scale matrix [M] as follows:

$$cir\left(\vec{X}_{ps}\right) = [M]\, cir\left(\vec{X}_{ms}\right) \qquad \text{(Eq. 14)}$$

$$[M] = cir\left(\vec{X}_{ps}\right) cir\left(\vec{X}_{ms}\right)^{-1} \qquad \text{(Eq. 15)}$$

Returning to the previous example solved using the Psuedo-Inverse method; we now attempt a solution using the Circulent matrix method. Recall:

$$[T_{ms}] = \begin{bmatrix} 450 \\ 400 \\ 365 \end{bmatrix} \qquad [T_{ps}] = \begin{bmatrix} 600 \\ 500 \\ 428 \end{bmatrix}$$

$$cir\left(\vec{T}_{ms}\right) = \begin{bmatrix} 450 & 365 & 400 \\ 400 & 450 & 365 \\ 365 & 400 & 450 \end{bmatrix}$$

$$cir\left(\vec{T}_{ps}\right) = \begin{bmatrix} 600 & 428 & 500 \\ 500 & 600 & 428 \\ 428 & 500 & 600 \end{bmatrix}$$

From Equation 15 above we derive the following transformation matrix:

$$[M] = \begin{bmatrix} 1.767 & -0.264 & -0.246 \\ -0.246 & 1.767 & -0.264 \\ -0.264 & -0.246 & 1.767 \end{bmatrix}$$

We now have derived a unique expression for the scale matrix [M] that represents a transformation from cir($\vec{X}_{ms}$) to cir($\vec{X}_{ps}$). Notice this [M] also satisfies the expression provided in Equation 12, which used the Psuedo-Inverse method. Another benefit to the circulent matrix method is the flexibility to interchange the rows of the state matrices provided the correlation between elements of the two matrices is maintained. One other extremely important characteristic of the Circulent matrix approach is that the two solution paths represented in Figure 3 produce the same results.

In contrast to the Psuedo-Inverse method, the Circulent matrix method has demonstrated the ability to derive unique transformation matrices using a single set of data points. In addition, it has also been demonstrated that the method has an inherent ability to meet the conditions required for convergence of the two solution paths. The Circulent matrix approach does require more complex matrix manipulations and a loss in intuitive comprehension of the process as a result.

## NICHE: NEW COMPENSATION MATRIX APPROACH:

The Psuedo-Inverse method provided an easily applied approach to predicting the performance of a product based upon the measured states of a model specimen, product specimen, and a model. Although relatively straightforward to apply, investigation into the method revealed that the derived scale and form transformation matrices were not unique representations of the transformations. This non-uniqueness results in predictions that are prone to errors, as we will see in the examples that follow. The Circulent matrix approach alleviated the uniqueness concern by deriving transformation matrices that are unique, but at a cost of increased mathematical complexity.

It is to our advantage to attempt to construct a material transformation matrix that maximizes the similarity characteristics inherent in the two systems, model specimen and product specimen. It is also to our advantage to attempt to separate the similarity characteristics from the dissimilar, or distorted, characteristics. This method attempts to satisfy both of these goals simultaneously. As an initial approximation to a solution using this method, we assume the scale transformation matrix [M] is a linear function. It is recognized that for the special case where two state vectors are not distorted due to similarity constraints (i.e. no dissimilarity), the transformation matrix between the two systems can be represented as a scaled identity matrix as shown below.

$$\begin{aligned} X_{ps,1} &= \lambda\, X_{ms,1} \\ X_{ps,2} &= \lambda\, X_{ms,2} \\ &\vdots \\ X_{ps,n} &= \lambda\, X_{ms,n} \end{aligned}$$

where λ represents a scalar quantity

$$\vec{X}_{ps} = \begin{bmatrix} \lambda & 0 & \cdots & 0 \\ 0 & \lambda & \cdots & 0 \\ \vdots & \vdots & \ddots & \vdots \\ 0 & 0 & \cdots & \lambda \end{bmatrix} \vec{X}_{ms}$$

$$\vec{X}_{ps} = \lambda [I] \vec{X}_{ms} \quad \rightarrow \quad [M] = \lambda [I]$$

However, the vast majority of modeled systems do contain a degree of distortion arising from material, geometry, loading conditions, or a number of other sources. Still the above derivation provides a good foundational starting point as the

only assumption made to this point is one of linearity of the transformation between the two considered systems. As a point of departure we seek an adjustment by way of a matrix perturbation, [δM], to the approximation described above which would allow the consideration of distorted systems in addition to well-scaled systems.

$$\vec{X}_{ps} = [M + \delta M]\vec{X}_{ms} \qquad \text{(Eq. 16)}$$

As previously stated, it is advantageous to derive a transformation matrix that both maximizes the similarity characteristics inherent in the two systems, captured in this formulation in the [M] matrix, and also isolates the distortion in the system [δM] to the maximum extent possible. In an attempt to accomplish this goal, we seek a least squares solution to maximize the diagonal components of the transformation matrix [M]. Maximizing the diagonal is equivalent to perturbing the transformation matrix in such a way as to maximize the similarity and thereby minimize the distortion in the transformation between the two state vectors. It is mathematically possible to fail to account for all the similarity in the matrix and thereby have it present itself as distortion components. A first order least squares solution maximizes the similarity in a linear system leaving the distortion behind. In addition to improving the accuracy of the prediction, this approach also offers greater insight into the characteristics of the system distortion, which offers the potential to analyze the anticipated error in our prediction. The derivation of the method is as follows:

We begin with the state vectors for the model and product specimens as shown below.

$$\vec{X}_{ms} = \begin{bmatrix} X_{ms,1} \\ X_{ms,2} \\ \vdots \\ X_{ms,i} \end{bmatrix} \qquad \vec{X}_{ps} = \begin{bmatrix} X_{ps,1} \\ X_{ps,2} \\ \vdots \\ X_{ps,i} \end{bmatrix}$$

A first order least squares solution takes the following form:

$$V = \begin{bmatrix} 1 & X_{ms,1} \\ 1 & X_{ms,2} \\ \vdots & \vdots \\ 1 & X_{ms,i} \end{bmatrix}$$

$$\vec{v} = \left(V^T \cdot V\right)^{-1} \cdot V^T \cdot X_{ps} \qquad \vec{v} = \begin{bmatrix} v_0 \\ v_1 \end{bmatrix}$$

It can be shown that the equation for $\vec{v}$ is always consistent and always produces a least squares straight line fit to the data [14]. The equation of the least squares line through the data points is written as follows:

$$y = (v_1)x + (v_0)$$

This equation provides the diagonal values of the [M] matrix from the $\nu_1$ term and also provides an additional correction term in the form of the $\nu_0$ term, considered the y-intercept in the above equation for the line:

$$[M] = \begin{bmatrix} v_1 & 0 & 0 & 0 \\ 0 & v_1 & 0 & 0 \\ 0 & 0 & \ddots & \vdots \\ 0 & 0 & \cdots & v_1 \end{bmatrix}$$

From Equation 16 we can rearrange terms and solve for the matrix perturbation [δM] as follows:

$$[\delta M] = \left(\vec{X}_{ps} - v_0 - [M]\vec{X}_{ms}\right)\vec{X}_{ms}^{+}$$

From this expression the value of [δM] is uniquely determined. Referring once again to Figure 3, we can now approximate the state of the product ( $\vec{X}_p$ ) from the following equation derived from Equation 7.

$$\vec{X}_p \cong [M + \delta M]\vec{X}_m$$

The compensation matrix approach has demonstrated both the ability to derive unique transformation matrices and presents itself in a form that allows straightforward observation of the process. A separation of the similarity contribution, provided by [M], from the distorted contributions, provided by [δM], also allows further analysis of the degree of distortion in the approximation. The following examples demonstrate the performance of the three ESMs and also offer a comparison with TSM as well.

## EXAMPLES:

### *1. Deflection of a Tapered Cantilevered Beam*

This example provides a direct comparison between the prediction capabilities of the TSM and ESM methods and also serves as evidence of the capabilities of the new Compensation method. The example is provided to demonstrate both the limitations of the TSM as well as the potential of the ESM to overcome those limitations. The goal in this example is to predict the deflection of an aluminum, tapered, cantilevered beam, supporting the beam weight and a transverse load acting

in the vertical direction and applied to the end of the beam as shown in Figure 4

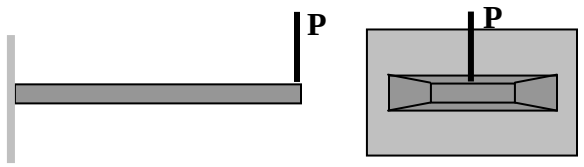


Figure 4. Tapered Cantilevered Beam.

The geometry, loading conditions, and material properties for the model specimen (ms), the product specimen (ps), the model (m), and the product (p) are listed in Table 2. Note the simplified geometry of the specimen beams, which are modeled using a representative rapid-prototyped polymeric material as non-tapered beams with a reduced length.

Table 2. Geometry, Loading, and Material Properties

| | Model Spec | Product Spec | Model | Product |
|---|---|---|---|---|
| Load (lb) | 1 | 10 | 1 | 10 |
| Modulus (Msi) | .45 | 10.5 | .45 | 10.5 |
| Density (lb/in$^3$) | .0433 | 0.1004 | .0433 | 0.1004 |
| Length (in) | 8 | 8 | 16 | 16 |
| Root Ht (in) | 0.125 | 0.125 | 0.375 | 0.375 |
| Root Width (in) | 1 | 1 | 2 | 2 |
| Tip Ht (in) | 0.125 | 0.125 | 0.2 | 0.2 |
| Tip Width (in) | 1 | 1 | 1 | 1 |

The deflection of the beams will result from a combination of the applied loading and the weight of the beam. From the information provided in Table 2 above, we can numerically calculate the deflection at any point along the length of the beam through direct integration of the moment and distributed load equations. By selecting five equally spaced points along the beams we derive state vectors representing discretized deflections for each of the four beam configurations as follows:

$$\vec{X}_{ms} = \begin{bmatrix} 0 \\ -.204 \\ -.742 \\ -1.5 \\ -2.368 \end{bmatrix} \qquad \vec{X}_{ps} = \begin{bmatrix} 0 \\ -.086 \\ -.313 \\ -.634 \\ -1.002 \end{bmatrix}$$

$$\vec{X}_{m} = \begin{bmatrix} 0 \\ -.039 \\ -.164 \\ -.389 \\ -.703 \end{bmatrix} \qquad \vec{X}_{p} = \begin{bmatrix} 0 \\ -.015 \\ -.066 \\ -.157 \\ -.286 \end{bmatrix}$$

Figure 5 shows the predicted beam deflections using the TSM and Psuedo-Inverse methods in relation to the theoretical beam deflection. Figure 6 shows the predicted beam deflections using the Circulent Matirx and Compensation Matrix methods again in relation to the theoretical beam deflection. Figure 7 shows the measured errors of the methods in comparison to the theoretical solution. As Figure 7 shows, the prediction of the beam deflection using both the TSM and Psuedo-Inverse methods results in substantial errors with the TSM resulting in approximately 17% error at the end of the beam. This error can be attributed to distortion in the system caused by failure of the tests to satisfy the similarity constraints of Equation 3. More precisely, if we consider the first two Π terms developed earlier in this paper:

$$\pi_1 |_m = \pi_1 |_p \quad \rightarrow \quad \left[EL^2 / P\right]_m = \left[EL^2 / P\right]_p$$
$$\pi_2 |_m = \pi_2 |_p \quad \rightarrow \quad \left[\rho L^3 / P\right]_m = \left[\rho L^3 / P\right]_p$$

Manipulation of these equations provides the following constraining ratios:

$$\left[E / \rho L\right]_m = \left[E / \rho L\right]_p$$

Given a model and a product with the same scale, the above constraints cannot be satisfied with the materials provided above due to the inequality of E/ρ for the model versus the product. The error is, therefore, anticipated. In contrast, the ESM methods provide increased prediction accuracy with the Compensation method resulting in the least error.

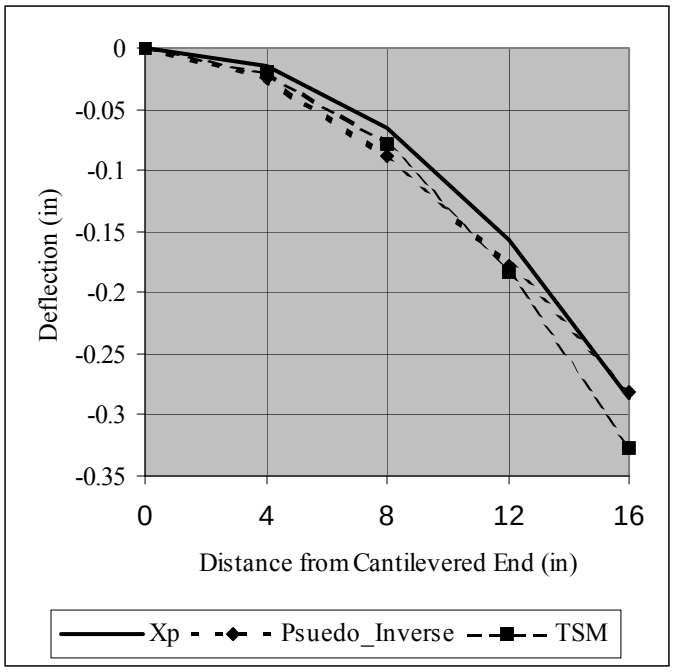


Figure 5. Predicted Beam Deflection using TSM and Psuedo-Inverse Methods.

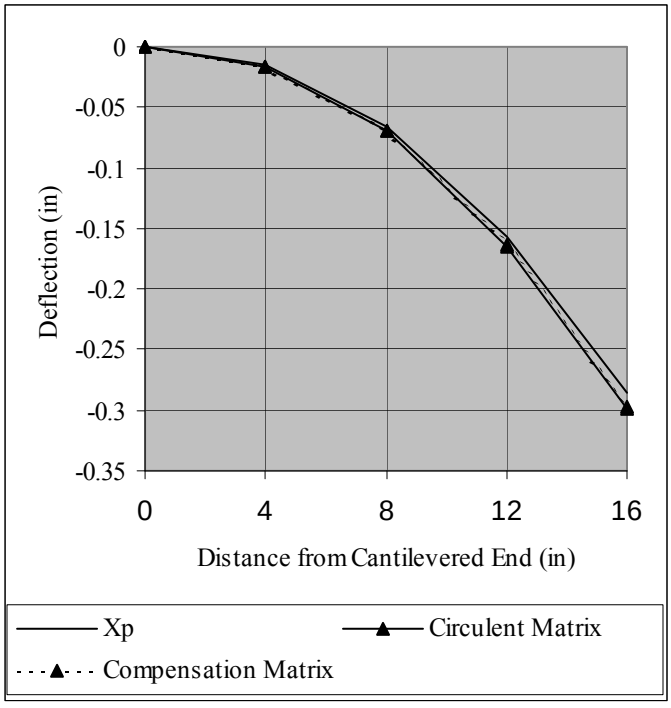


Figure 6. Predicted Beam Deflection using circulent Matrix and Compensation Matrix Methods.

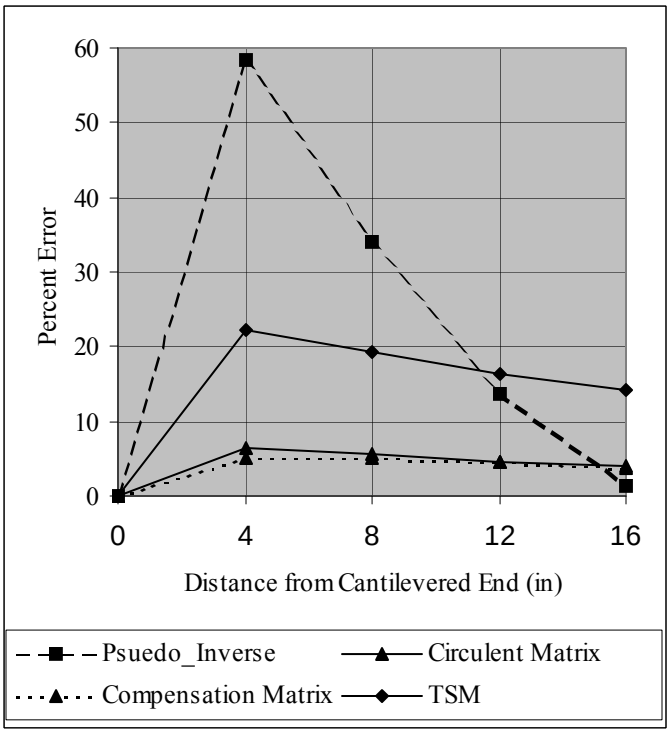


Figure 7. Error in Predicted Beam Deflection.

In the development of the current ESMs, it is recognized that two paths exist to get from the state of the model specimen ( $\vec{X}_{ms}$ ) to the state of the product ( $\vec{X}_{p}$ ) as shown in Figure 3. It is assumed that the paths produce identical results based upon the assumption that the specimen pair and the model-product pair are designed according to the same similarity constraints and, therefore, that [M] = [M'] and [G] = [G']. As this paper shows and the example above demonstrates, satisfying all the similarity constraints is often not feasible and the inclusion of polymeric materials and complex geometry only serves to increase the difficulty in obtaining a non-distorted system. The recognized distortion in a system invalidates the assumption that [M] = [M'] and [G] = [G'] and, therefore, the assumption that the two solution paths produce identical results.

Research to date has shown significant inconsistencies in the degree of accuracy capable with the different ESM solution methods [12]. The example above shows almost exact correlation between deflection of the product beam and the prediction using the Compensation Matrix approach, the most accurate method developed yet to derive transformation matrices for the prediction of state vectors from specimen and model state vectors. Similar experimental studies have also shown drastic differences and levels of inaccuracy from the different ESMs when applied to example problems where the actual solution has either been determined analytically or determined from empirical testing.

### 2. *Steady-State Thermal Conduction Problem [12]*

In this experimental example, conducted by Cho, et al. [12], we present the results of an empirical study of the prediction of the thermal conduction of a product based upon the measured temperatures of a model and specimen pair at corresponding points within the objects as shown in Figure 8. The state vectors representing the measured temperatures of the four variants (model specimen, product specimen, model, product) are shown below. The prediction results for Psuedo-Inverse method, the Circulent Matrix method, and Compensation Matrix method are shown in Figure 9. Figure 10 shows the error in each of the methods compared to the actual measured temperatures of the product.

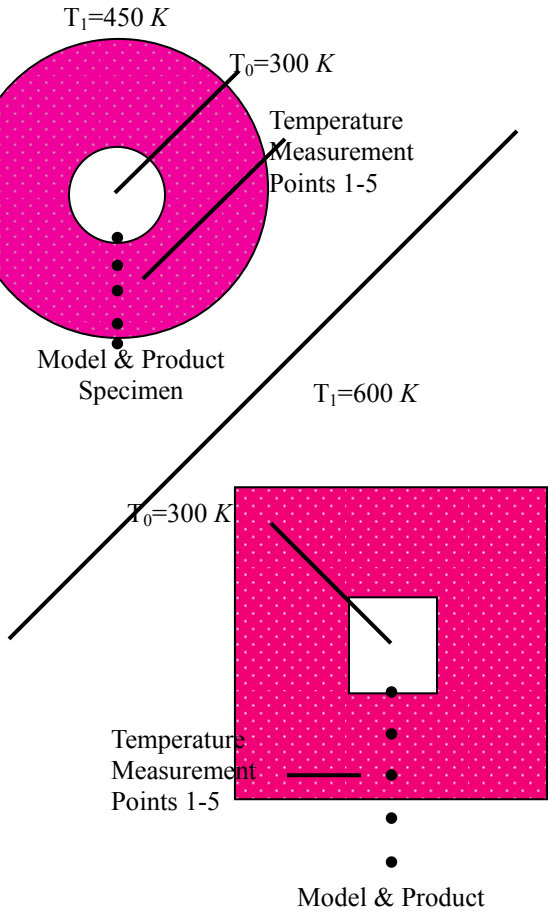


Figure 8. Temperature Boundary Conditions for Specimen Pair, Model and Product.

$$[T_{ms}] = \begin{bmatrix} 300 \\ 330 \\ 365 \\ 400 \\ 450 \end{bmatrix} \qquad [T_{ps}] = \begin{bmatrix} 300 \\ 360 \\ 428 \\ 500 \\ 600 \end{bmatrix}$$

$$[T_{m}] = \begin{bmatrix} 300 \\ 306 \\ 333 \\ 378 \\ 450 \end{bmatrix} \qquad [T_{p}] = \begin{bmatrix} 300 \\ 312 \\ 365 \\ 460 \\ 600 \end{bmatrix}$$

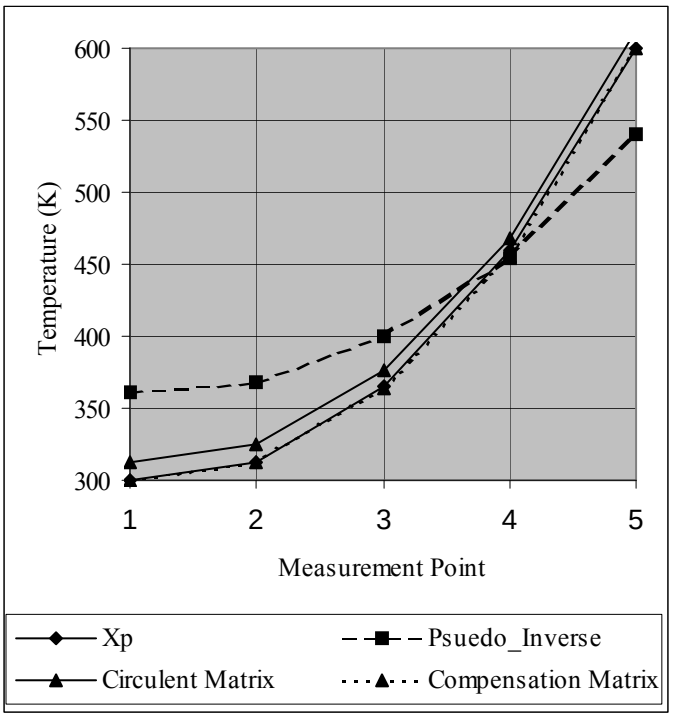


Figure 9. Product Temperature Predictions

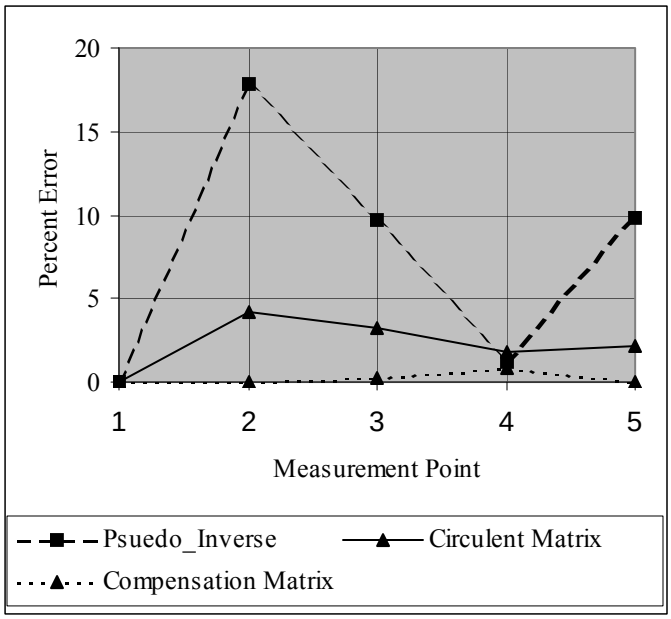


Figure 10. Error in Prediction Methods.

As Figure 9 and Figure 10 show, the temperatures predicted by the Circulent and Compensation Matrix methods are significantly more accurate than the Psuedo-Inverse method. In addition, from this example we see the Circulent and Compensation Matrix methods produce almost identical results with the Compensation method proving slightly better.

## CONCLUSIONS

In this paper, we have endeavored to present the latest in ongoing research directed toward enhancing the empirical predictive capabilities of a new generation of dimensional analysis based methods. To date the methods have shown a significant ability to manipulate material and geometric transformation mapping to the prediction of product performance parameters using simple test specimens and a product representative scale model. The ease of manufacturing the specimens and model using rapid-prototyping technology

## ACKNOWLEDGMENTS

The work reported in this document was made possible, in part; by a grant from the National Science Foundation Graduate Research Traineeship and the University of Texas June and Gene Gills Endowed Faculty Fellowship. Any opinions, findings, or recommendations are those of authors and do not necessarily reflect the views of the sponsors.

## REFERENCES

1. Becker, H.A., *Dimensionless Parameters Theory and Practice*. 1976, London: Applied Science Publishers LTD.
2. Cho, U., Wood, K.L., and Crawford, R.H., "Novel Empirical Similitude Method for the Reliable Product Test with Rapid Prototypes", *Proceedings of the 1998 ASME DETC*, Atlanta, GA, 1998, ASME.
3. Wall, M.B.e.a., "Making Sense of Prototyping Technologies for Product Design", *ASME 3rd International Conference on Design Theory and Methodology*1991, ASME.
4. Bridgman, P.W., *Dimensional analysis, by P.W. Bridgman*. 1946, New Haven,: Yale University Press.
5. Birkhoff, G., *Hydrodynamics; a study in logic, fact, and similitude*, Rev. [i.e. 2d] ed. 1960, Princeton: Princeton University Press.
6. Palacios y Martínez, J., *Dimensional analysis*. 1964, New York: Macmillan; St. Martin's Press.
7. Murphy, G., *Similitude in engineering*. 1950, New York,: Ronald Press Co.
8. Bridgman, P.W., *Dimensional analysis*. 1931, New Haven: Yale University Press.
9. Barr, D., "Consolidation of Basics of Dimensional Analysis", *Journal of Engineering Mechanics, ASCE*, 1984. **10**(9): p. 1357-1375.
10. Langhaar, H.L., *Dimensional analysis and theory of models*. 1980, Huntington: R. E. Krieger Pub. Co.
11. Huntley, H.E., *Dimensional analysis*. 1951, New York: Rinehart & Co.
12. Cho, U., "Novel Empirical Similarity Method for Rapid Product Testing and Development", in *Mechanical Engineering*. 1999, University of Texas at Austin: Austin TX.
13. Strang, G., *Linear Algebra and Its Applications*. 1988: Harcourt Brace Jovanovich, Inc.
14. Nakos, G. and Joyner, D., *Linear Algebra with Applications*. 1998: Brooks/Cole Publishing.